Int. J. Electrochem. Sci., 11 **(2016)** 6110 – 6125, doi: 10.20964/2016.07.80

International Journal of
ELECTROCHEMICAL
SCIENCE
www.electrochemsci.org

The Influence and Mechanism of Corrosion on AZ31B Magnesium Alloy in 1,2-propanediol Engine Coolant

Zi-wen Wang[1], *Wei Bai*[1,*], *Yan Yang*[2], *You Wu*[1],*Chang-Wei Su*[1], *Jun-Ming Guo*[1]

[1] Key Laboratory of Resource Clean Conversions in Ethnic Regions, Yunnan Minzu University, Kunming, 650500, PR China
[2] Natural rubber and coffee Quality Supervision and Testing Center of Yunnan Nong-Ken
[*]E-mail: bw369852147@qq.com

Received: 17 March 2016 / *Accepted:* 17 May 2016 / *Published:* 4 June 2016

Corrosion mechanism of AZ31B magnesium alloys in 1,2-propanediol coolant has been studied using polarization curves, EIS, SEM and SEM- EDS. Magnesium alloy can be formed a stable and tight protective film in foundation liquid, which can easily be destroyed in the simulation solution. Little change in temperature on magnesium alloy reaction mechanism. But serious hydrogen evolution reaction occurs at high temperament on magnesium alloy surface in basis solution.

Keywords: Magnesium alloys; polarization curves; EIS; 1,2-propanediol coolant

1. INTRODUCTION

Magnesium alloy has been hailed as the most development and application of green engineering materials in 21st century by materials experts. Because of its low density, high thermal conductivity and stiffness, excellent electromagnetic, mechanical processing and damping properties, excellent ability to cast and recovery capacity [1-4], the magnesium alloy material is considered to be a promising project future in the automotive, aerospace, electronics and entertainment industries [5,6]. With the deepening of energy saving, environmental protection, safety concept, auto parts manufacturing materials will increasingly be substituted by magnesium alloy. If the magnesium alloy can become a new engine materials, will be more effective in reducing the weight of vehicles and to achieve the goal of green energy. It is well known that the electrochemical activity of magnesium alloys is higher [7-11], resulting in their high corrosion rate. In general, the magnesium alloys have good corrosion resistance in alkaline solution [12-16], but active in the acidic or neutral environment, which indicates that the pH value of the corrosion resistance of magnesium alloys significant effect.

Therefore, a lot of researches on magnesium and its alloys have been concentrated in the alloying elements, surface modification and corrosion effects on microscopic [17-19]. There are many factors that can cause corrosion of magnesium alloys, liked in different environments will affect the rate of corrosion and corrosion mechanism.

Among them, the corrosion mechanism of magnesium alloys in engine coolant needs to be further explored. According to the American Society for Testing and Materials standard ASTM-D 3306-00, the coolant is divided into four types: glycol concentrate, concentrate propylene glycol, ethylene glycol dilution (150% by volume) and diluted with propylene glycol (150% by volume). Propylene glycol coolant as one of the environment-friendly coolant is the most striking [20, 21], this type of coolant with incomparable superiority than water - glycol coolant. It is known that anhydrous propylene glycol based coolant freezing point as low as -68 ℃, and the boiling point of up to 187 ℃ witch have veritable performance in anti-boiling and frost resistance.

Currently, few research corrosion mechanism of magnesium alloys in 1,2-propanediol / water system, and the high cost of waterless - 1,2-propanediol can not do so popular, in order to reduce costs, there are many worthy attempts to consider and explore the1,2-propanediol based coolant which join the water in [22-24]. Pardo and others have been studied the corrosion behavior of magnesium alloys in a variety of commercial cooling liquid inside, and the results showed that compared with aluminum, magnesium alloy corrosion and serious [25]. But the corrosion of water - 1,2-propanediol coolant for magnesium alloy engine is relatively serious, which required a lot of theoretical research for achieving universal access and the further developing.

2. EXPERIMENTAL METHODS

2.1. Composition of the specimens

Preparation of the working electrode from the AZ31B magnesium alloy having the following composition (weight%): Si 0.069%, Mn 0.42%, Zn 1.12%, Ni0.00072%, Al 3.12%, Cu0.0069% and Mg: balance.

2.2. Medium

The formulation of 1,2-propanediol / water liquid was: 30%(vt) propylene glycol and 70%(vt) water. The formulation of 1,2-propanediol simulation liquid was: 1,2-propanediol content of 30%, corrosive solution formulated with reference to standard of ASTM-D1384-96 [26] (sodium sulphate (148mg / L), sodium chloride (165mg / L), sodium bicarbonate (138mg / L) and water balance).

2.3. Electrochemical procedure

All electrochemical measurements were performed in a thermostatic three-electrode system. Before measuring the working electrode with the resin encapsulation and 1cm2 of magnesium alloy exposed area. In each measurement, the sample surface with 100# to 1200# sandpaper polishing, washed with double distilled water, degreased with acetone and dried in warm air [27]. Saturated calomel electrode (SCE) and a platinum electrode been used as a reference and an auxiliary electrode. In all experiments, the magnesium alloy of the working electrode is allowed to take place after it reaches a stable open circuit potential (OCP) for two hours. The Tafel polarization curves were polarizing from -250 mV up to 1000 mV. SCE were selected using a scan rate 0.5 mV/s. The excitation signal amplitude of AC impedance measurement was 10mV and frequency was 0.1 ~ 10^5Hz. Analysis of impedance spectra with Zview software. Electrochemical tests are used CS350 electrochemical workstation (Wuhan QUASAR Instrument Co., Ltd.) and using DKZ series electric heated water bath (Shanghai Heng Scientific Instrument Co.) to constant temperature at 25℃ and 88℃.

2.4. pH tests

pH tests carried out in the 1,2-propanediol / water liquid and 1,2-propanediol simulation liquid, immersing in different time. pH tests were surveyed by PHS-3C, (Shanghai Electronics Scientific Instrument Co., Ltd., China).

2.5. Scanning electron microscopy (SEM)

Four samples were immersed in different media and temperature for 24 hours, removed AZ31B magnesium alloy sheets and dry immediately, and then examined by using scanning electron microscope with an accelerating voltage of 20 kV (Holland yielding XL30 ESEM-TMP).

2.6. Energy Dispersive Spectrometer (EDS)

In this thesis, EDS was used to analyze the elemental composition of the material, the type and content on microanalysis. The samples have been immersed in base fluid and simulate coolant 24 hours at different temperatures.

3. RESULTS AND DISCUSSION

3.1. Electrochemical experiments

3.1.1. Potentiodynamic polarization curves

In order to study the corrosion mechanism of low levels of 1, 2-propanediol coolant for magnesium alloys, we selected 30% by volume 1,2-propanediol content to research. Fig. 1 and Fig. 2 were magnesium alloy polarization curves at different soaking time in 1,2-propanediol/water-based liquid (based liquid) and 1,2-propanediol simulation liquid. On the whole, changing the soaking time, it has changed the cathode and the anode, where the anode greater change. In based liquid cathode changed should been hydrogen evolution reaction[28], anodic reaction was the dissolution process of magnesium alloys which produced Mg $(OH)_2$, these two processes had a greater impact on the pH of the solution.

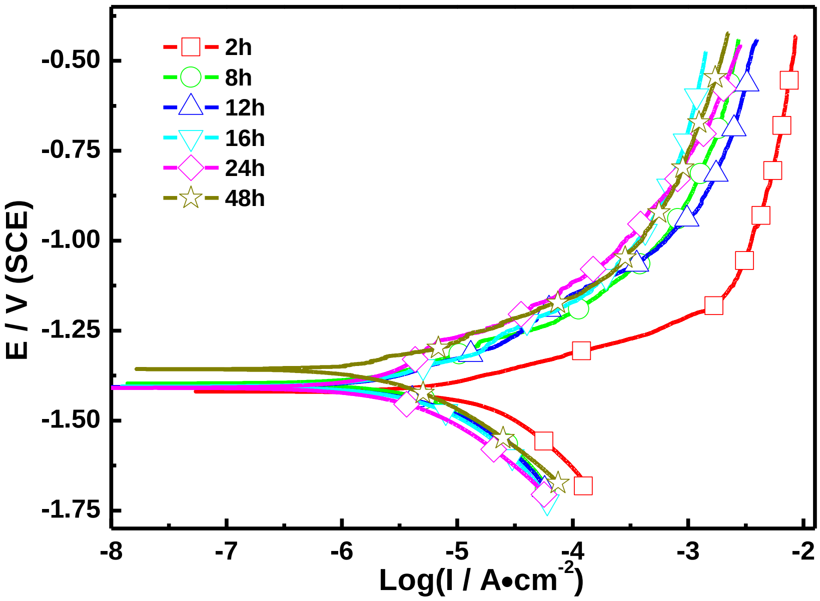

Figure 1. Magnesium alloy polarization curves at different soaking time in 30% 1,2-propanediol / water liquid at 25 ℃.

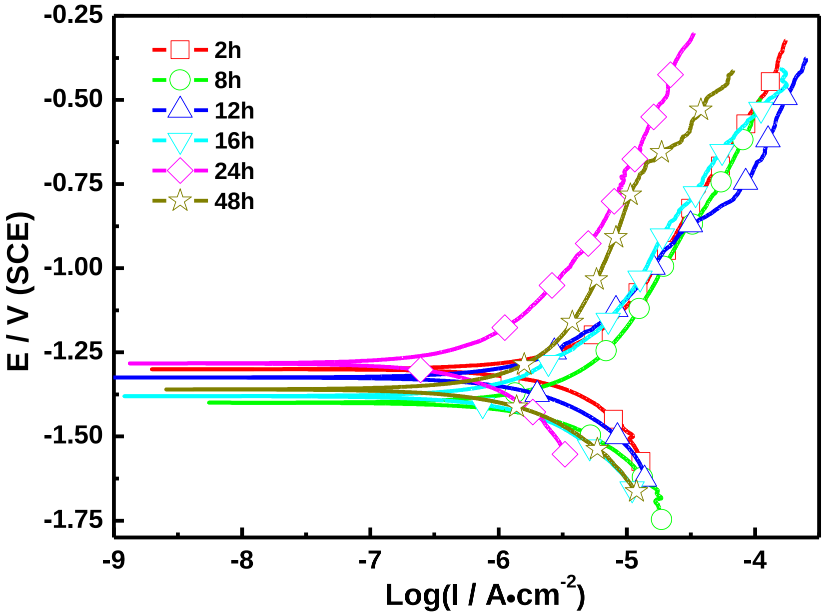

Figure 2. Magnesium alloy polarization curves at different soaking time in 1,2-propanediol simulation liquid at 25 ℃.

Table 1. Polarization curve parameters of AZ31B magnesium alloy is immersed in different times of 30% 1,2-propanediol / water and 1,2-propanediol simulation liquid at 25 ℃ .

Medium	t / (h)	E_{corr} / V	b_c / (mV·dec^{-1})	b_a / (mV·dec^{-1})	i_{corr} / (μA·cm^{-2})
1,2-propanediol / water liquid	2	-1.3041	159.56	183.98	1.3788
	8	-1.4018	124.48	157.91	95.901
	12	-1.3305	154,70	205.40	96.916
	16	-1.3781	138.39	156.37	48.350
	24	-1.2828	141.60	98.09	17.870
	48	-1.3600	132.20	193.84	54.960
Medium	t / (h)	E_{corr} / V	b_c / (mV·dec^{-1})	b_a / (mV·dec^{-1})	i_{corr} / (μA·cm^{-2})
1,2-propanediol simulation liquid	2	-1.4191	199.57	118.74	12.862
	8	-1.3969	178.68	171.00	3.9243
	12	-1.4065	171.48	155.39	3.6412
	16	-1.4052	189.18	169.65	3.7718
	24	-1.4079	127.25	180.72	1.5271
	48	-1.3575	185.16	128.84	2.5664

In Table 1, the i_{corr} of based liquid proof magnesium alloy changed during the start 12 hours soaked constantly corroded, from intense to slow, gradual corrosion products attached to the surface of magnesium alloy, forming a layer of protection film, soaking to 24 hours, since the corrosion current reaches a minimum value, a protective film rupture after 24 hours, corrosion and continues to intensify, but not before violent shows only a small range of protective film rupture. Table 1, the corrosion current density value in based liquid proof that magnesium alloy continuously corroded during the first 12 hours, from severe to slow, gradual corrosion products adhering magnesium alloy surface to form a protective film, soaking the first 24 hours, the protective film ruptured, the degree of corrosion began to increase, but not violent than before which indicated that the protective film was only to rupture a small range. From 24 hours to 48 hours was magnesium alloy surface protective film to partial rupture process. It can be seen that: in solution consisting of 1,2-propanediol and water, in a short time, the surface of the protective film was firm. Fig. 2 was corrosion process of simulated cooling liquid for magnesium alloy .From Fig. 2 can be seen with increasing immersion time, changed in the anode and the cathode was not obvious, but compared with Fig. 1, the corrosion has became violent. This showed that the addition of corrosive ions exacerbated the extent of corrosion, but made the system stable. Corrosive ions main role was to destroy the protective film which has formed by corrosion products in the surface of magnesium alloy, making the overall corrosion reaction can be stable. But the corrosion current changed in Table 1 of simulated liquid medium can be seen the corrosion reaction process was a cycle process of: accumulation of corrosion products formed a film - corrosion ion damaged film - corrosion products accumulate on magnesium alloy surface. According to the corrosion current data shows that due to the corrosive ions was added, this cycle process has been began before soaked since the beginning. But the reaction can be stably carried out due to the corrosive ions added.

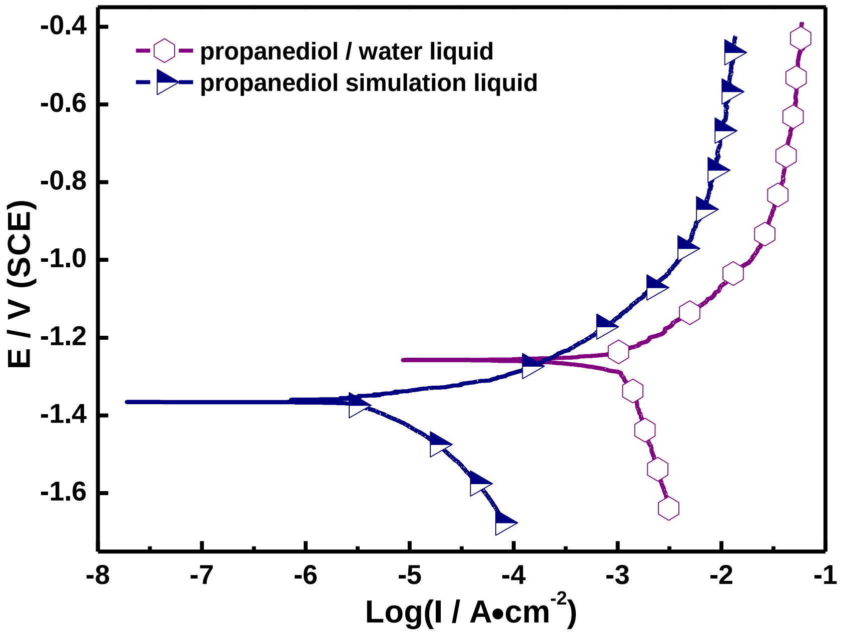

Figure 3. Polarization curves of AZ31B magnesium alloy in 1,2-propanediol/water liquid and 1,2-propanediol simulation liquid medium 2 hours at 88 °C.

Fig. 3 showed that the magnesium alloy corrosion in based liquid was more intense than in analog coolant on high temperature during short time. Tafel slope of the cathodic (b_c) in base fluid was greater than in analog liquid, which consistent with the results of Fig.1 and Fig. 2. This proved that the same basic mechanism of increasing the reaction temperature for two systems. According to the cathode segment of polarization curve from Fig. 3 in based liquid, we speculated that this phenomenon caused by hydrogen evolution reaction [28]. And the high temperature for the hydrogen evolution reaction in base liquid was more severe impact, resulting in high temperature, corrosive was more serious in foundation liquid during the first 2 hours.

Table 2. Polarization curve parameters of AZ31B magnesium alloy was immersed in 1,2-propanediol / water and 1,2-propanediol simulation liquid 2 hours at 88 ℃ .

Medium	E_{corr} / V	b_c / (mV·dec^{-1})	b_a / (mV·dec^{-1})	i_{corr} / (μA·cm^{-2})
1,2-propanediol / water liquid	-1.2631	243.00	130.38	624.17
1,2-propanediol simulation liquid	-1.3668	163.69	58.46	4.0267

From Table 2, the corrosion current density can also get the same conclusion. Anodic Tafel slope (b_a) changes were also consistent with the low temperature, can be seen from Table 2, the anode metal dissolution process in based liquid more fast. This was because the hydrogen evolution reaction, increasing the electron transfer rate and a large number of OH^- reacted with Mg to product $Mg(OH)_2$, while magnesium alloy gathered a large OH^- to exclude most of the corrosive ions offensive in short time. Changes in corrosion current density values can explain the severity of corrosion in basis liquid. Taken together, due to the sharp increase in the hydrogen evolution reaction, leading to initial corrosion was more intense at high temperatures in base liquid.

3.1.2. Electrochemical impedance spectroscopy (EIS)

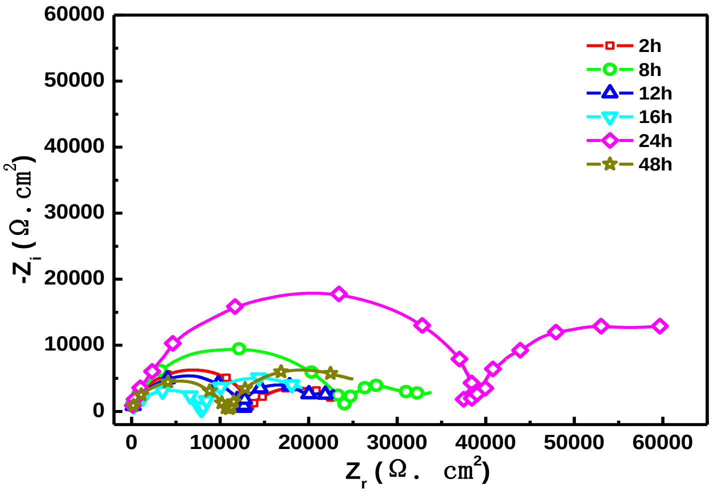

Figure 4. Nyquist plots of magnesium alloy impedance spectra at different soaking time in 30% 1,2-propanediol / water liquid at 25 ℃.

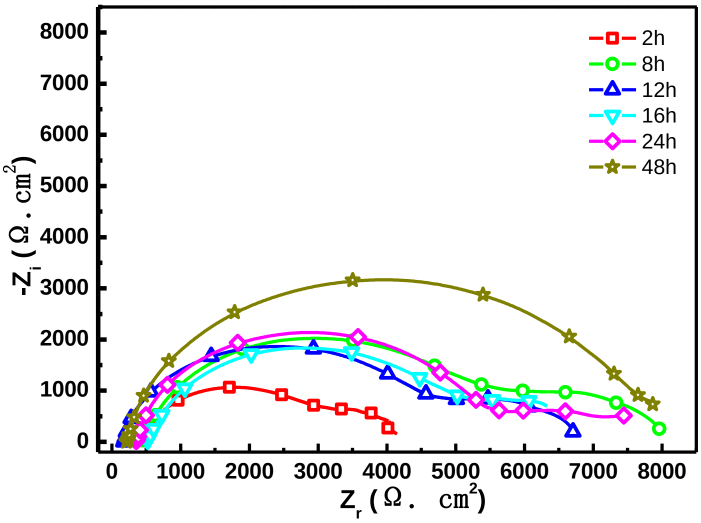

Figure 5. Nyquist plots of magnesium alloy impedance spectra at different soaking time in 30% 1,2-propanediol simulation liquid at 25 ℃.

Fig. 4 and 5 are Nyquist curve of magnesium alloy in based liquid and simulation liquid at 25℃. Both figures are depressed capacitive loops, which were often attributed to the working electrode surface roughness and unevenness [29]. This behavior is not the influence of corrosive ions, but the nature of the activation control of a charge transfer reaction process. Constant phase angle element CPE which in circuit instead of a pure double layer capacitor was introduced to give a more accurate fitting, and CPE_{f-P}, CPE_{dl-P} values are within 0.5-1 in Table 3[30].

Table 3. The electrochemical parameters obtained from EIS plots for magnesium alloy in 1,2-propanediol / water liquid and 1,2-propanediol simulation liquid at 25 ℃.

Medium	t / (h)	R_s (Ω .cm^2)	CPE_{f-P}	CPE_{f-T}（μF·cm^{-2}）	R_f（Ω· cm^2）	CPE_{dl-P}	CPE_{dl-T}（μF· cm^{-2}）	R_{ct}（Ω· cm^2）
1,2-propanediol / water liquid	2	32.39	0.95	$3.001\ e^{-3}$	13038	0.64	22.71	12954
	8	22.02	0.90	$6.125\ e^{-3}$	23325	0.59	41.07	12230
	12	19.80	0.92	$4.794\ e^{-3}$	12156	0.68	31.64	12361
	16	22.69	0.86	$1.001\ e^{-2}$	7717	0.66	32.74	18465
	24	15.85	0.91	$5.135\ e^{-3}$	38391	0.64	26.34	45239
	48	29.36	0.92	$4.458\ e^{-3}$	10418	0.64	33.83	22104
Medium	t / (h)	R_s (Ω .cm2)	CPE_{f-P}	CPE_{f-T}（μF· cm^{-2}）	R_f（Ω· cm^2）	CPE_{dl-P}	CPE_{dl-T}（μF· cm^{-2}）	R_{ct}（Ω· cm^2）
1,2-propanediol simulation liquid	2	413.6	0.83	17.8	2879	0.91	687	789.2
	8	439.5	0.84	14.6	5240	0.88	8783	2103
	12	196.0	0.94	12.6	3888	0.68	5039	2993
	16	497.1	0.83	15.4	4800	0.96	1484	1232
	24	352.6	0.90	11.3	5112	0.83	1916	1775
	48	230.6	0.92	11.3	7178	0.59	1560	1884

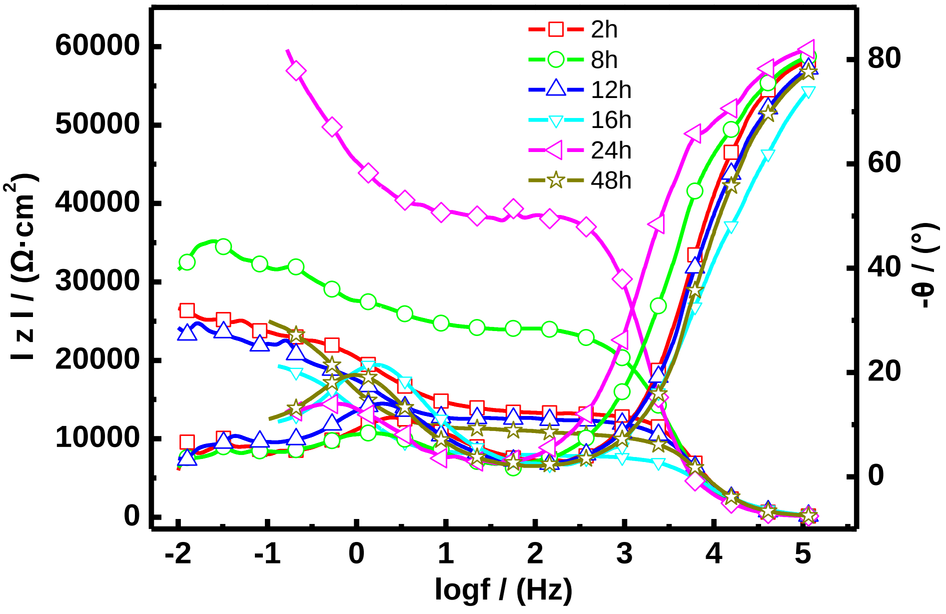

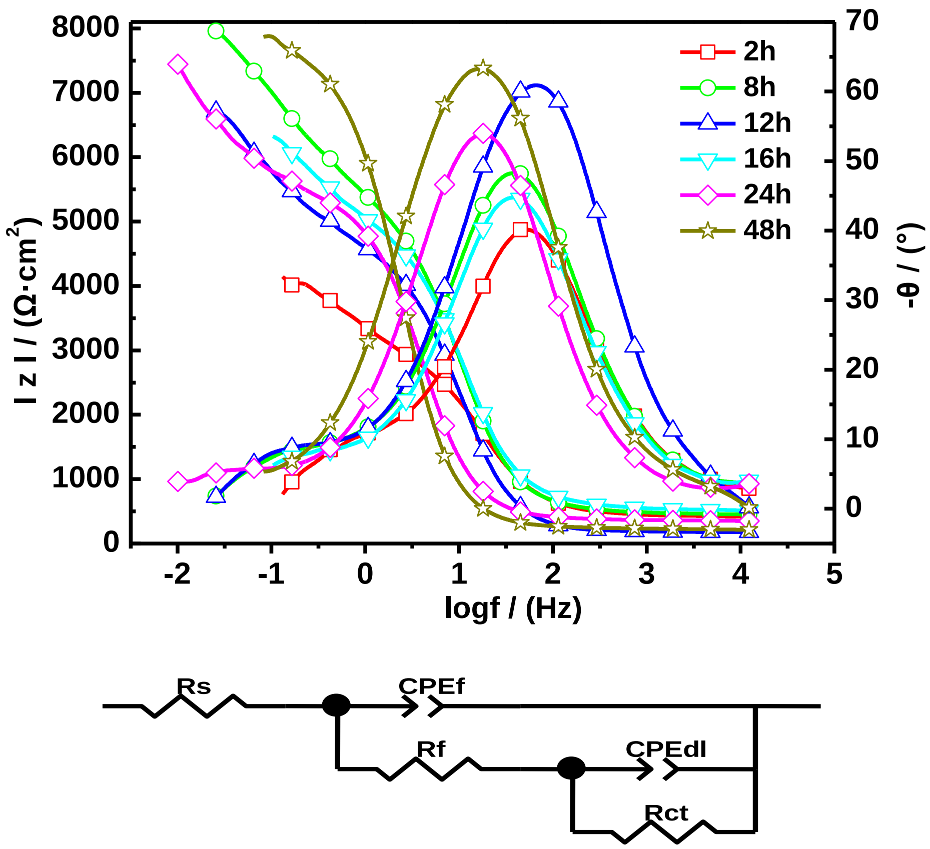

Figure 6. Bode plots of magnesium alloy in1,2-propanediol / water liquid and 1,2-propanediol simulation liquid at 25 ℃. The equivalent circuit used to fit the impedance spectra which obtained from magnesium alloy in both the appropriate conditions.

Table 4. The electrochemical parameters obtained from EIS plots for magnesium alloy in 1,2-propanediol / water liquid and 1,2-propanediol simulation liquid at 88 ℃.

Medium	R_s (Ω .c^2)	CPE_{f-P}	CPE_{f-T}（ μF· cm^{-2} ）	R_f（ Ω· cm^2 ）	CPE_{dl-P}	CPE_{dl-T}（ μF· cm^{-2} ）	R_{ct}（ Ω· cm^2 ）
1,2-propanediol / water liquid	0.1	0.88	9.7	20.30	0.82	1677	65.34
Medium	R_s (Ω .cm^2)	CPE_{f-P}	CPE_{f-T}（ μF· cm^{-2} ）	R_f（ Ω· cm^2 ）	CPE_{dl-P}	CPE_{dl-T}（ μF· cm^{-2} ）	R_{ct}（ Ω· cm^2 ）
1,2-propanediol simulation liquid	73.63	0.93	142.8	2874	0.57	48.8	3400

All EIS spectra can use two equivalent circuits in Fig. 6 to analyze and fitted well with our experimental results. R_p represents polarization resistance, R_s represents ohmic resistance of solution and R_{ct} is a charge transfer resistance, which value is a measure of electron transfer on the surface, and inversely proportional to the corrosion rate.

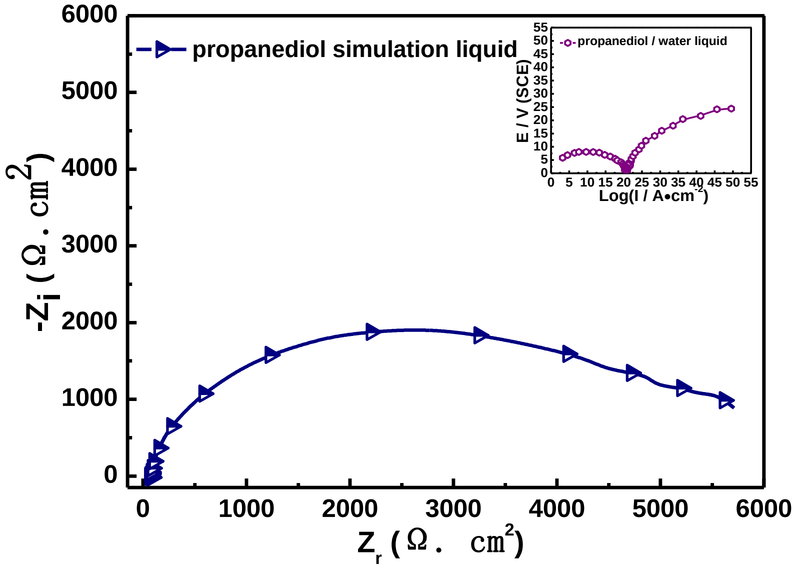

Figure 7. Nyquist plots of magnesium alloy impedance spectra at different soaking time in 30% 1,2-propanediol / water liquid 2 hours at 88 ℃.

In Fig. 4, the magnesium alloy surface formed a layer of film, as immersion time increase, this layer of protective film has not disappeared. R_p changed in Table 3, can be seen, the protective film with the increase of time, which says there have been OH^- system to destroy the membrane structure, but the new generation of $Mg(OH)_2$ has become the new protective film, which is protected by a magnesium alloy is a process of self-contradiction. Can be seen from the R_p values in Table 3 that before the 16 hours the protective film was constantly been generated - breakdown - generation, after the 16 hours has been to generate a protective film until 24 hours when polarization resistance value was reached. The law of this process was consistent with polarization curve. Table 3 were shown greater resistance of R_{ct} in based liquid, indicating the degree of membrane rupture is not large. Fig. 5 becomes an arc, indicating that the addition of corrosive ions, preventing $Mg(OH)_2$ was adsorbed on the surface of magnesium alloy, but into the solution. This is related with corrosive anion constantly attacked magnesium alloy surface and $Mg(OH)_2$ was attracted by Na^+ in the solution. However, after 24 hours, the charge transfer resistance became larger, indicating that corrosive anions had been depleted. In Table 3, R_{ct} reached its maximum in the first 48 hours but the degree of corrosion still serious than in the foundation liquid.

Compared Nyquist and bode diagram at different temperatures of the two systems can found that the corrosion reaction were accelerated in two solutions under high temperature. Soaked for 2 hours under high temperature, corrosion rate of the base fluid very quickly, it can be seen in Table 4 R_{ct} and R_p are very small. But the basic reaction mechanism of magnesium alloy surface is basically consistent with the low temperature. The EIS to fit also can use equivalent circuit in Figure 6. As can be seen from Fig. 7, the corrosion rate of the two solutions are fast, electrochemical workstation can only test corrosion in short-term.

3.2. pH results

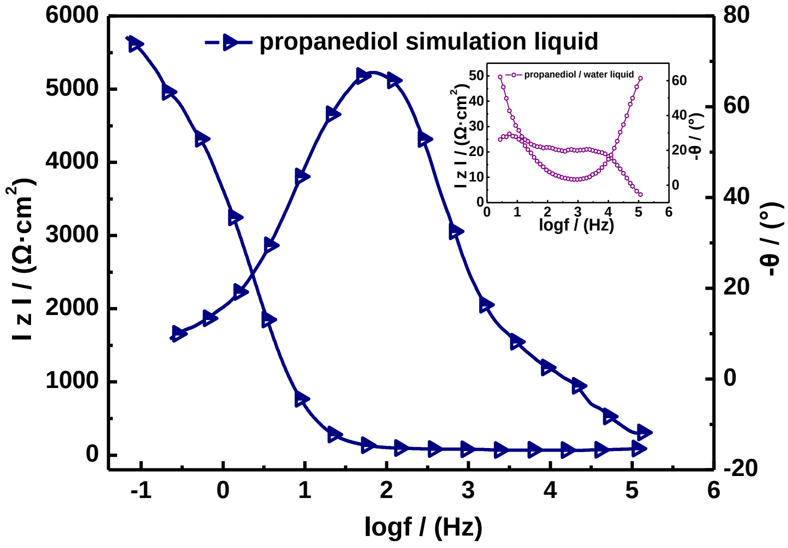

Figure 8. Bode plots of magnesium alloy in1,2-propanediol / water liquid and 1,2-propanediol simulation liquid 2 hours at 88 ℃.

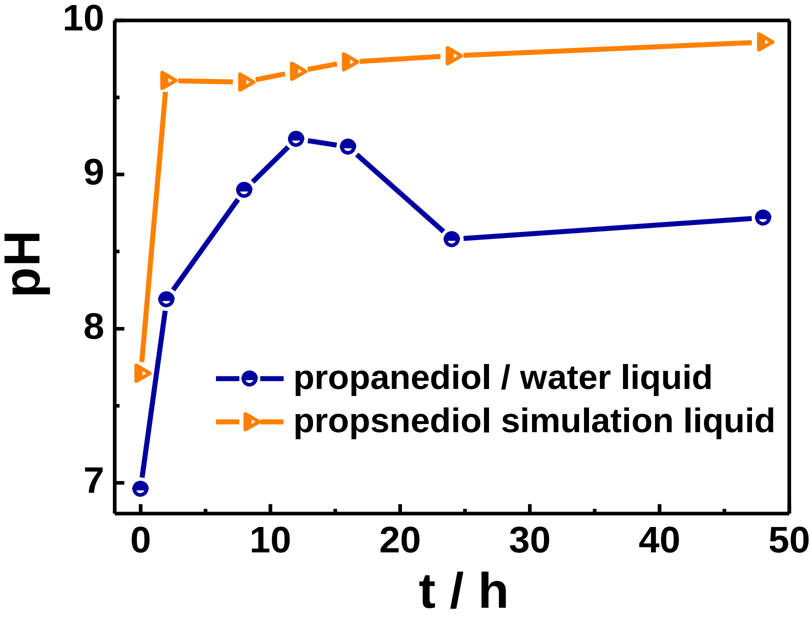

Figure 9. The relationship between soak time and pH in 1,2-propanediol / water liquid and 1,2-propanediol simulation liquid at 25 ℃.

Fig. 9 indicated that the relationship between time and pH immersion in based liquid and simulation solution at 25 ℃. The first line shows that with the increase of immersion time, pH first increased and then decreased. When the magnesium alloy soaked in based liquid, pH of the solution has been increasing at 12 hours ago, but after the 12 hours, soaking time increased, pH decreased. After 24 hours the pH stabilized at about 8.7. This indicates that 24 hours ago the Mg continuous dissolved in the solution to $Mg(OH)_2$ which was gradually to attach magnesium alloy's surface to prevent the Mg further oxidation. But after the 12 hours, the system did not generated a lot of $Mg(OH)_2$, but H^+ not completely to generate hydrogen, resulting in lowering the pH value of the solution. The second line can be seen, pH of the solution in a short time to stabilize at around 9.6, which is relatively high. This shows that the sodium sulphate (148mg / L), sodium chloride (165mg / L) and sodium bicarbonate (138mg / L) were added have been changed the reaction mechanism of the system. Because of CO_3^{2-}, $SO4^{2-}$ and Cl^- going to destroy the layer of $Mg(OH)_2$ on protective film, so the system reacted in an environment of mutual restraint until balance[31,32].

pH changes in the based fluid system were very large after to rise temperature. According to our observation, a lot of bubbles adhered to the surface of magnesium alloy. Combined with polarization curve, we think it that caused by violent hydrogen evolution reaction. Obviously, hydrogen evolution reaction was suppressed after the addition of corrosive ions, which was related to the pH and temperature. Within the first two hours, the solution pH variations are large, indicating that the high temperature accelerates the corrosion of the reaction system. But ph has been in a steady growth in simulation solution, which showed that magnesium alloy was corrosion continuously. By the late pH declined in based fluid system, which we hypothesized that it was the same reason with low temperatures.

3.3. Scanning electron microscopy (SEM) analysis

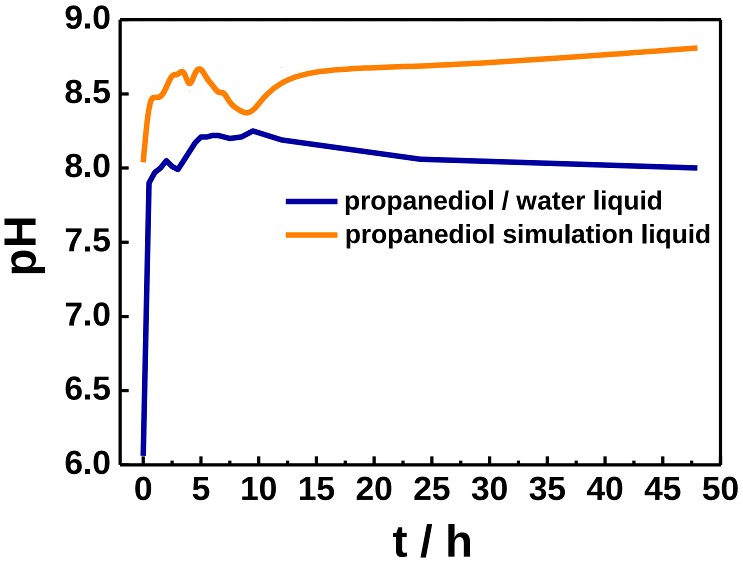

Figure 10. The relationship between soak time and pH in 1,2-propanediol / water liquid and 1,2-propanediol simulation liquid at 88 ℃.

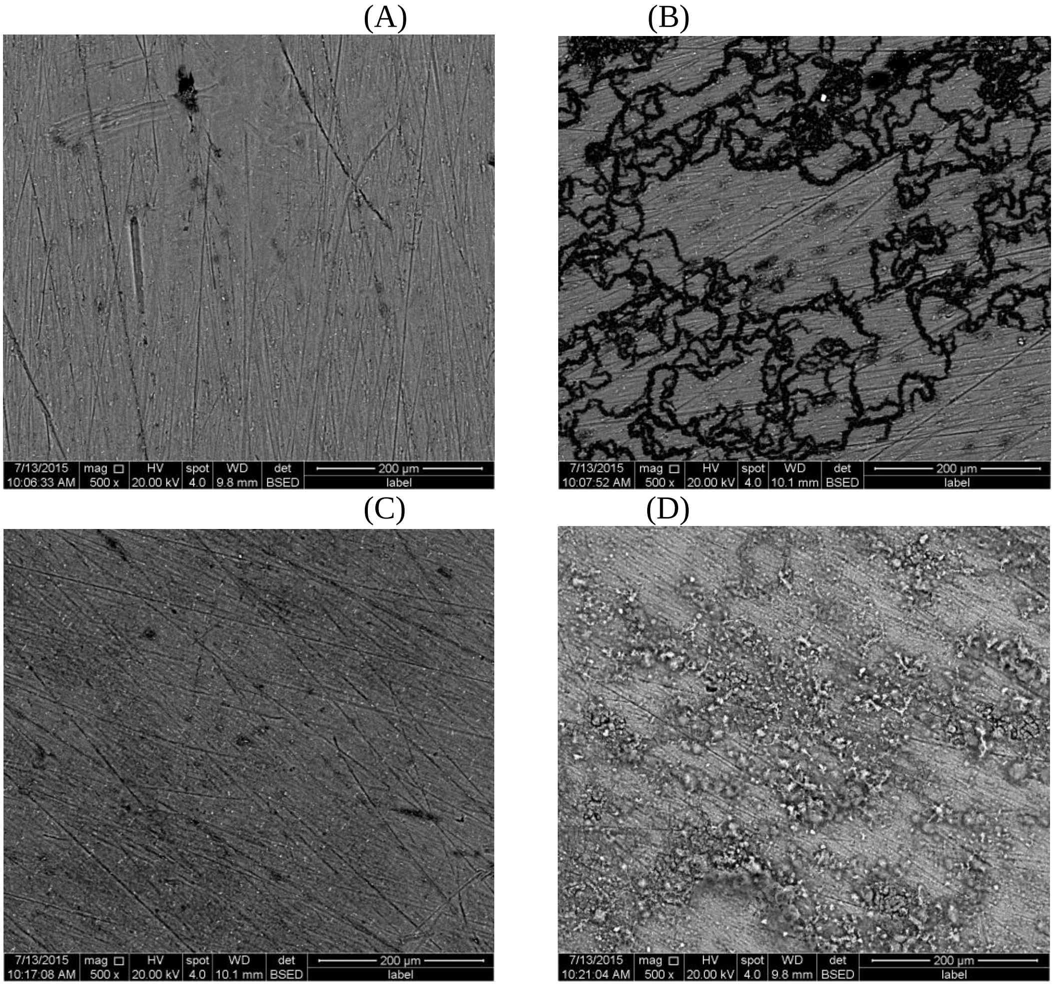

Figure 11. Electron micrographs of magnesium alloy in 30% 1,2-propanediol / water (A) , analog coolant (B) at 25 ℃ and in 30% 1,2-propanediol / water (C) , analog coolant (D) at 88 ℃.

In order to understand the impact of changing temperature and composition of the solution for magnesium alloys, magnesium alloy were soaked in different study conditions for 24 hours and then used scanning electron microscope to observe. (A) was the scan of magnesium alloy to immerse in based liquid at 25 ℃, which can be seen magnesium alloy surface corrosion was not serious. Because of we can see polish line and on metal surface had formed a layer of protective film what was presumably $Mg(OH)_2$. (B) was the scan of magnesium alloy to immerse in 1,2-propanediol at 25 ℃. The figure shows the surface of magnesium alloy attached a lot of strip corrosion products which been inferred that CO_3^{2-} , SO_4^{2-} and Cl^- destroyed the original protective film, they changed the magnesium alloy surface adsorption electric double layer electric field distribution, resulting in a deeper corrosion[31,32].

(C) changed the temperature ratio than (A), the comparison showed that the temperature increasing destructed of the $Mg(OH)_2$ but not serious because the surface looks fairly smooth, and not a lot of corrosion products. (D) changed the reaction temperature than (B) which can be seen from the figure that the reaction product changes and corrosion more severely, the surface has been very rough, difficult to see the original metal surface. SEM results further show that, for a long time, temperature and corrosive ions increased degree of corrosion.

3.4. Energy Dispersive Spectrometer analysis

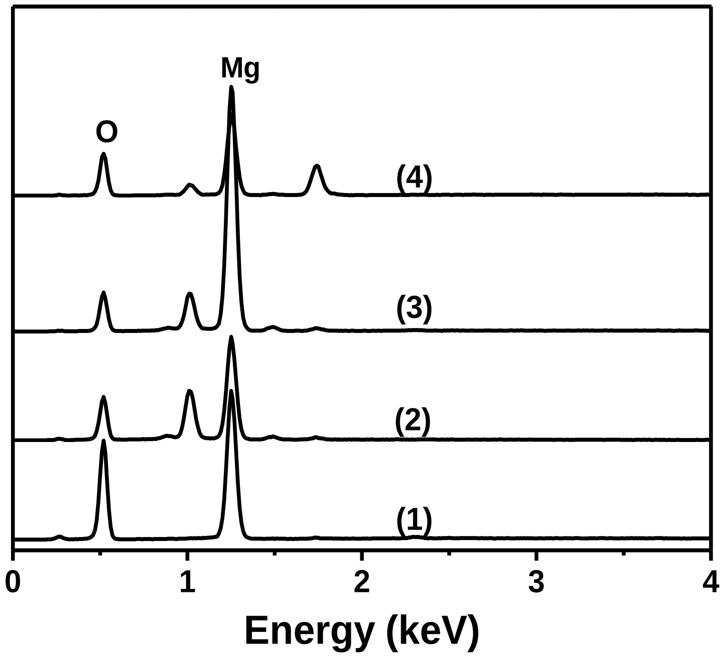

Figure 12. The EDS of magnesium alloy was soaked in 1,2-propanediol simulation liquid (1) , 1,2-propanediol / water liquid (2) at 25 ℃ and in 1,2-propanediol simulation liquid (3) , 1,2-propanediol / water liquid(4) at 88 ℃.

Table 5. The elemental composition obtained from EDS for magnesium alloy soaked in1,2-propanediol simulation liquid and 1,2-propanediol / water liquid at different temperament for 24 hours.

T/ (℃)	Medium	Element	Weight percent	Percentage atom
25	1,2-propanediol simulation liquid	O	53.91	63.99
		Mg	46.09	36.01
	1,2-propanediol / water liquid	O	40.12	50.45
		Mg	59.88	49.55
88	1,2-propanediol simulation liquid	O	31.91	41.59
		Mg	68.09	58.41
	1,2-propanediol / water liquid	O	32.65	42.41
		Mg	67.35	57.59

Fig.12 is the element types and content of corrosion surface on AZ31B magnesium alloy. Magnesium and magnesium alloy surface will form a layer of $Mg(OH)_2$ in water as a main component of the medium. Articles have described the formation of corrosion products and the stability of the deposited films had been destroyed at high temperatures and corrosive ions are added. Fig.12 shows, different environments, covering the surface of magnesium alloy corrosion product is not the same after a long soak. In table 5, percentage of element indicate that the magnesium alloy surface corrosion products mainly was $Mg(OH)_2$ which soaked in the simulated liquid at 25℃, other environments mainly were MgO. $Mg(OH)_2$ is not stable after prolonged immersion and high temperature will accelerate the $Mg(OH)_2$ into MgO which finally deposited to the metal surface.

The percentage of the elements in table 6 shows that $Mg(OH)_2$ accounts for the main components in fluid simulation at a low temperature. Because of the corrosive ions was added, so that the capacity of dense MgO / $Mg(OH)_2$ protective film attached magnesium alloy surface to reduce. These lead to the corrosion rate of Mg increases and continue to produce large amounts of $Mg(OH)_2$. Finally, $Mg(OH)_2$ accounts for the majority for the sample surface in this condition. Since all experimental parameters did not reflect or detected 1,2-propanediol involved in the reaction, we think 1,2- propanediol is stable in this test. According to former study concluded the reaction mechanism [33]:

$2Mg(s) \rightarrow 2Mg^{+}(aq) + 2e$ (Anodic reaction)

$2H^{+} + 2e \rightarrow H_2$ (Cathodic reaction)

$2Mg^{+}(aq) + 2H_2O(aq) \rightarrow 2Mg^{2+}(aq) + OH^{-}(aq) + H_2$ (Chemical reaction)

$Mg(s) + H^{+} + H_2O \rightarrow Mg(OH)_2(s) + H_2$ (Overall reaction)

$Mg(OH)_2 \rightarrow MgO + H_2O$

4 CONCLUSIONS

Corrosion mechanism of magnesium alloys in 1,2-propanediol coolant been summarized as follows:

(1): Magnesium alloy oxide film produced in the 1,2-propanediol / water system is not easily broken at high temperature.

(2): In 1,2-propanediol / water system added corrosive substances can slow the hydrogen evolution on magnesium alloy surface at high temperatures.

(3): After a long soak, a large number of $Mg(OH)_2$ was converted to MgO adhering to the metal surface.

ACKNOWLEDGEMENT
This work was financially supported by Natural science fund item of China（51161025， 51561032）, Natural science fund item of Yunnan province （2011FZ173), Program for Innovative Research Team (in Science and Technology) in University of Yunnan Province (2011UY09), Teaching reform project of Yunnan Province （2013027）.

References

1. S.F. Liu, L.Y. Liu, L.G. Kang, *J. Alloys Compd.* 450 (2008) 546–550.
2. F.H. Froes, D. Eliezer, E. Aghion, *JOM* 50 (1998) 30–34.

3. Y. Uematsu, T. Kakiuchi, M. Nakajima, *Mater. Sci. Eng.* 531 (2012) 171–177.
4. G. Song, A. Atrens, D. Stjohn, J. Nairn, Y. Li, *Corros. Sci.* 39 (1997) 855–875.
5. Z.M. Shi, G. Song, A. Atrens, *Corros. Sci.* 48 (2006) 1939–1959.
6. S. Feliu Jr., C. Maffiotte, J.C. Galván, V. Barranco, *Corros. Sci.* 53 (2011) 1865–1872.
7. R.B. Alvarez, H.J. Martin, M.F. Horstemeyer, M.Q. Chandler, N. Williams, P.T. Wang, R. Augusto, *Corros. Sci.* 52 (2010) 1635–1648.
8. A.N. Chamos, S.G. Pantelakis, V. Spiliadis, *Mater. Des.* 31 (2010) 4130–4137.
9. G.L. Song, A. Atrens, *Adv. Eng. Mater.* 1 (1999) 11–33.
10. R. Xin, B. Li, L. Li, Q. Liu, *Mater. Des.* 32 (2011) 4548–4552.
11. P.L. Bonora, M. Andrei, A. Eliezer, E.M. Gutman, *Corros. Sci.* 44 (2002) 729–749.
12. Y.G. Ko, S. Namgung, D.H. Shin, *Surf. Coat. Technol.* 205 (2010) 2525–2531.
13. H. Chen, G.H. Lv, G.L. Zhang, H. Pang, X.Q. Wang, H.J. Lee, S.Z. Yang, *Surf. Coat. Technol.* 205 (2010) S32–S35.
14. S. Durdu, M. Usta, *Appl. Surf. Sci.* 261 (2012) 774–782.
15. X. L, X.Y. Liu, B.L. Luan, *Appl. Surf. Sci.* 257 (2011) 9135–9141.
16. E.E. Demirci, E. Arslan, K.V. Ezirmik, Ö. Baran, Y. Totik, İ. Efeoglu, *Thin Solid Films* 528 (2013) 116–122.
17. Q. Wang, Y.H. Liu, S.J. Fang, Y.L. Song, D.W. Zhang, L.N. Zhang, C.F. Li, *Mater. Charact.* 61 (2010) 674–682.
18. T.T. Yan, L.L. Tan, B.C. Zhang, K. Yang, J. Mater. *Sci. Technol.* 30 (2014) 666–674.
19. H.G. Liu, Q. Xu, D.M. Xiong, B. Lin, *C.L. Vacuum* 89 (2013) 233–237.
20. B. Casale, A.M. Gomez, Method of hydrogenating glycerol, *US Patent* 5214219, 1993.
21. J. Chaminand, L. Djakovitch, P. Gallezot, P. Marion, C. Pinel, C. Rosier, *Green Chem.* 6 (2004) 359.
22. Z. Shi, P.K. Mallick, R.C. McCune, S. Simko, F. Naab, *Magnesium Technology 2010, TMS2010,* pp. 173–179.
23. P. Zhang, X. Nie, D.O. Northwood, *Surface Coatings Technol*, 203 (2009) 3271–3277.
24. L.H. Han, X.Y. nie, H. Hu, Mater. *Technol.* 24 (2009) 170–173.
25. A. Pardo, M.C.Merino , A.E.Coy , R.Arrabal , F.Viejo , E. Matykin . *Corrosion Science.* 50 (2008) 823–834.
26. ASTM D1384-97, *1999 annual book of ASTM Standards*, Vol.15.05, ASTM, Philadelphia, p. 9.
27. Li X H, Mu G N. *Applied Surface Science,*2005, 1254-1259.
28. Genevieve Baril, Nadine Pebere. *Corrosion Science,*2001,43:471-484.
29. S.S. de Assunção Araújo Pereira, M.M. Pêgas, T.L. Fernández, M. Magalhães, T.G.Schöntag, D.C. Lago, L.F. de Senna, E. D'Elia, *Corros. Sci.* 65(2012) 360–366.
30. M. Behpour, S.M. Ghroreishi, N. Soltani, M. Salavati-Niasari, M. Hamadanian, A.Gandomi, *Corros. Sci.* 50 (2008) 2172–2181.
31. Cowan K G,Harrison J A. *Electrochem Acta* 1979,24: 301-308.
32. R. Lindstrom.J.E.sevenson.J.Hanzen. J . *Electrochem. Soc.* 2002, 149(4):13103. 357-268.
33. F.-H. Cao, V.-H. Len, Z. Zhang,and J.-Q. Zhang. *Russian Journal of Electrochemistry,* 43(2007) 837–843.